

# Interference mitigation and power consumption reduction for cell edge users in future generation networks

---

## ABSTRACT

Network densification of small cells (SCs) and macro cells (MCs) is a novel and promising solution proposed to tackle the increasing demand for higher data rates in 5G heterogeneous networks (HetNets). Unfortunately, the interference that occurs between these closely packed SCs and their high-power consumption has generated huge problems facing the 5G HetNets. In this work, a new soft frequency reuse (SFR) scheme is proposed to reduce the interference and increase the network throughput. The proposed scheme uses the soft frequency reuse (SFR) for on/off switching of the SCs according to their interference contribution rate (ICR) values. It solves the interference problem of the closely packed SCs by dividing the cell region into edge and centre zones. Moreover, SCs on/off switching tackles the high-power consumption problem and enhances the power efficiency of the 5G network. Furthermore, this work tackles the irregular shape nature problem of 5G HetNets and compares between two different proposed shapes for the center zone of the SC, existing irregular and proposed circular shapes. Additionally, the optimum radius of the center zone, which maximizes the total system data rate, is obtained. A comparative analysis of power consumption, data rate and power efficiency were performed between NSFR model, SFR model and the proposed model. The results show that the proposed model has low power consumption compared to the other two methods, and consequently, high data rate which implies that the interference level is low, and a high-power efficiency. The results obtained show that the interference mitigation handled by the proposed scheme improves by approximately 22%.

*Keywords: 5G Cellular Network; Small Cells; Macro Cells; SFR Model; NSFR Model*

## 1. INTRODUCTION

An average of 0.01% of new user equipment is added to telecommunications networks on a daily basis[1]. The cumulative effect of this increase on devices which are connected to 5G (5thGeneration) network pose some pertinent issues in the network system which warrant system upgrade in terms of capacity, efficient energy consumption, and well-regulated data rates. Over the years, series of research have been conducted on wireless telecommunications, diffraction loss, path length and other related issues[2, 3]. Furthermore, research has shown that the number of devices connected to the 5G network will be between 10 and 100times higher than what is obtainable in 4G networks and the data rates will increase up to 10 Gbps [1, 4].

There is a prediction that by the year 2030, the communication sector will contribute to about 51% of the global electricity consumption[5]. Consequently, researchers have invested quality efforts to investigate and develop some approaches to manage the upcoming

overhead in the communication sector and by extension, the power sector. Such approaches include; Massive Multi-Input Multi-Output (MIMO) systems[6]and Millimetre Wave (mm-wave)[7]technologies. These researchers[8] made significant breakthrough in their approach, which portrayed small cells as a novel technique with high efficiency in 5G services. However, their approach still leaves some foot print of challenges in area of power consumption within the small cells and high interference between the cells. In order to address the power consumption problem, another group of researchers [9]carried out survey on open issues in energy efficiency of 5G network and the group in[10] implemented sleep mode switching in small cells. Several degrees of sleep depth were also proposed in[11]. These sleep strategies were only effective where there are macro cells. Small cells wake up when macro cells are overloaded. Invariably, the sleep mode strategy does not function where there is no macro cell. A sleep mode-based resource allocation strategy was proposed by [12]. In their method, interference map was formed to select disabled femtocell, but the shortcoming of this method is the inability to update the map on disabled femtocells which result in non-optimal solution.

The shortcomings of the aforementioned techniques which include high level of complexity especially for antenna designs, and time investment in assembly line arouse the interest in this research to investigate and propose a novel method to ameliorate the core system metrics while keeping its design and implementation simple and efficient.

The aim of this research is to reduce interference mitigation and power consumption in 5G networks. To achieve this aim, the following objectives were followed: developed network cell segmentation scheme for interference mitigation and power reduction for cell edge users in 5G heterogeneous network using interference contribution rate technique for small cell switching control; developed and evaluated shape-based model using cluster vertices formation for small cell; developed centre zone determination mechanism for various shapes of network zones; computed the optimal radius of the zone centroid hence, improved the overall system data rate; and benchmarked the proposed method with other existing methods.

## 2. METHODOLOGY

### 2.1 Model Overview

The model simulation and validation were performed using Matrix Laboratory (MATLAB). The selected parameters adopted for the simulation are presented in Table 1. In the simulation environment, macro cells were created and they contained small cells according to the model design presented in Figure 1. The target network area had users' equipment arbitrarily distributed.

**Table 1. Simulation parameters**

Parameter	Value
Total number of small cells	200
Total number of user equipment	100 – 1000
Small cell idle index ( $\phi$ )	0.52
Resource segment bandwidth	200kHz
Total number of resource segments	100
Overall bandwidth	20MHz

Base station power amplifier efficiency ( $\eta$ )	0.52
Noise power spectral density	$-180\text{dBm/Hz}$
Power consumption gradient based on load ( $\sigma$ )	6
Path loss between small cell and user equipment	$150.2 + 40.1 \log_{10}(d)$ (db); $d$ represents the distance (Km) between the considered small cell and user equipment
Transmission power of small cells	$20\text{dBm}$

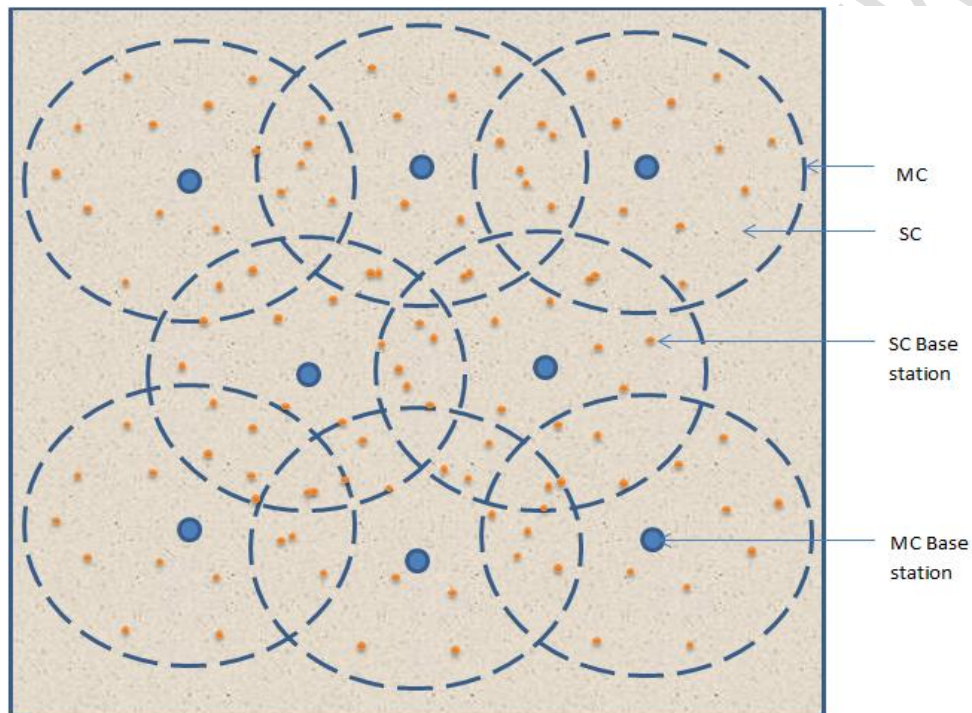


**Figure 1. Heterogeneous network system model**

This research used experimental methodology for interference mitigation and power consumption reduction for cell edge users in 5G network using Network cell Segmentation scheme (NetSc), with the heterogeneous network as the network type considered. In the simulation environment, macro cells were created and they contain small cells (SCs) as presented in Figure 1. The target network area had user equipment arbitrarily distributed. The small cells were mounted within a network region marked as macro cells (MCs) which were designed to operate within the low frequency band to achieve a wide coverage area. On the other hand, high frequency band formed the operating region of the SCs and this is to ensure that a substantial network capacity is obtained.

The frequency band variation between SCs and MCs cancels out any interference that may exist between them. In order to avoid drift in coverage area during SC switching, MCs must be kept alive always. As a backup solution, an effective handover scheme is required for all user equipment (UE) contained in the dead SC. If there are available channels in MC, the

user equipment in the dead SC should be moved immediately to the MC. SCs can either be in ON state or OFF state. During OFF (sleep) state, user equipment continuously receives discovery signal by the active SCs while they transmit their channel state to the connected SC. The assumption that governs this information exchange is that the user equipment is within the communication area of the SC. In this research, SCs switching are not considered to be arbitrary, hence, it is assumed that the scheduler manages the allocation of sub-bands to the SCs as well as their switching control. However, if the scheduler fails, the MCs oversee the information collation from the SCs and control the sub-band sharing and SCs switching.

Considering the model in Figure 1, it is impossible to compute transmission power of any small cell without considering the signal-to-noise ratio as well as interference from neighbouring cells. In general engineering terms, signal to noise ratio (SNR) can be defined as the ratio of the useable power level to noise level and can be expressed mathematically as:

$$SNR = \frac{P_0}{N_0} \quad (1)$$

Where,  $P_0$  denotes output power level,  $N_0$  denotes interference or noise level measured in dB.

Consider a collection of SCs and a collection of user equipment which will be represented by  $\chi_{SC}$  and  $\psi_u$ , respectively. The concept in Equation 1 can be applied to obtain the signal to noise ratio for any user equipment within a small cell. Before the computation of signal to noise ratio, the small cell switching concept is considered since the small cells can either go on or off. Let the small cell switching factor be denoted by  $\delta_{sw}$  and its value at any given time is regulated by Equation 2 and signal to noise ratio for user equipment within a given small cell can be computed by Equation 3[13].

$$\delta_{sw} = \begin{cases} 1 & \text{if SC is on} \\ 0 & \text{if SC is off} \end{cases} \quad (2)$$

$$SNR_{SC,UE} = \delta_{sw} \cdot G \cdot \left( \frac{P_{SC}}{\sum P + N_0 BW} \right) \quad (3)$$

Where,  $G$  denotes gain,  $P_{SC}$  is the transmission power of the small cell,  $P$  is the overall transmission power,  $N_0$  denotes the noise element, and  $BW$  denotes the bandwidth assigned to the user equipment.

A specific quantity of resources must be allocated to user equipment according to the user's required data rate. This is necessary to avoid bridge in quality of service (QoS). In any given small cell, the data rate of user equipment in that cell can be calculated as given in Equation 4 [13].

$$DR = BW_{RS} \cdot \log_2(1 + SNR_{SC,UE}) \quad (4)$$

Where,  $RS$  denotes the resource segment and  $BW_{RS}$  denotes the bandwidth of the resource segment.

In order to get the least data rate needed by the user equipment, the knowledge of the resource segment for that equipment is required, and this can be computed as the ratio of

minimum data rate needed by the user equipment to the data rate of the user equipment within the considered small cell. This is represented mathematically as Equation 5[13].

$$N_{RS} = \text{ceil} \left( \frac{DR_{UE_{min}}}{DR} \right) \quad (5)$$

Where,  $DR_{UE_{min}}$  represents the smallest data rate needed by the user equipment.

The down scaling operator (ceil) in Equation 5 is applied to ensure that the least integer is returned by the function. In any given small cell, the data rates can be computed as the summation of data rates of user equipment as in Equation 6[13].

$$DR_{SC} = \sum DR_{UE} \quad (6)$$

By applying Shannon's computation methods Equation 6 can be modified to Equation 7.

$$DR_{UE} = BW \cdot \log_2 e^0 + BW \cdot SNR_{SC,UE} \quad (7)$$

The reduction in noise power will definitely increase  $SNR_{SC,UE}$ , and consequently, increase in data rate will be realized. The overall power in the small cell in active mode can be computed as in Equation 8[13].

$$P_{SC_{on}} = P_{TH} + \alpha_L \cdot \alpha_{amp} \cdot P_{nom} \quad (8)$$

Where,  $P_{TH}$  is the threshold power,  $\alpha_L$  is the power loss factor,  $\alpha_{amp}$  is the power amplification factor, and  $P_{nom}$  is the nominal power consumption.

Although small cell can be in sleep state, power consumption can still be obtained but negligible. In sleep state, power consumption in small cell can be computed as in Equation 9[13].

$$P_{SC_{off}} = P_{TH} \cdot \varepsilon \quad (9)$$

Where,  $\varepsilon$  represents the depth of idleness of the small cell.

Thus, the overall power consumption of a small cell is computed as Equation 10 [13].

$$P_{SC_T} = \sum_{t_1}^{t_{max}} P_{SC_{off}} + (1 - \varepsilon) \sum_{t_1}^{t_{max}} P_{SC_{on}} \quad t_1 < t_{max} \quad (10)$$

Where,  $t_1$  is any initial time that could be considered and  $t_{max}$  is any final time that could be considered, and the constraint  $t_1 < t_{max}$  must be strictly followed.

The first part of the Equation 10 computes the total time when the small cells stay off. Similarly, the total power during the active period is computed on the second part of the Equation 10. The lower and the upper time boundaries allow the power consumption to be computed for any range of time. The expanded form of Equation 10 can be expressed as Equation 11[13].

$$P_{SC_T} = \sum_{t_1}^{t_{max}} P_{TH} \cdot \varepsilon + (1 - \varepsilon) \sum_{t_1}^{t_{max}} \alpha_L \cdot \alpha_{amp} \cdot P_{nom} \quad t_1 < t_{max} \quad (11)$$

Transmission power  $P_{nom}$  of a small cell which is a member of the second part in Equation 11 can be computed as Equation 12 [14].

$$P_{nom} = \sum N_{RS} \frac{\sigma P_{max}}{\eta N_{RS_{max}}} \quad (12)$$

Where,  $\sigma$  denotes the residual power consumption as a result of load,  $P_{max}$  denotes the highest transmission power by small cell,  $N_{RS_{max}}$  denotes the maximum number of resource segments, and  $\eta$  denotes the base station's amplifier efficiency.

In order to minimize interference in the target 5G network, this research applies some novel techniques to regulate the attenuation level for frequency handover above sensitivity level. The interference effect of any small cell  $i_{SC}$  can be expressed as the ratio of small cell induced interference power to the sum of reference signal power of all active user equipment. This can be computed as in Equation 13[14].

$$i_{SC} = \frac{P_{SC} \cdot G_{SC}}{\sum P_{UE} \cdot G_{UE}} \quad (13)$$

Where,  $P_{SC}$  is the transmission power of the small cell,  $G_{SC}$  is the gain in small cell,  $P_{UE}$  is the transmission power of user equipment,  $G_{UE}$  is the gain in user equipment.

Let  $\mathbb{C}$  denote the correction factor to regulate the quantity of handover small cell switching, Equation 13 can be rewritten as Equation 14 [13].

$$i_{SC} = \frac{P_{SC} \cdot G_{SC}}{(\sum P_{UE} \cdot G_{UE}) \cdot \mathbb{C} \cdot N_{UE}} \quad (14)$$

Where,  $N_{UE}$  is the quantity of user equipment in small cell.

From Equation 14, when  $\mathbb{C} \cdot N_{UE}$  increases, it implies that the quantity of user equipment has increased. This will consequently reduce  $i_{SC}$  as well as the certainty level of the small cell off state.

## 2.2 Network Cell Segmentation (NetSc) Scheme

This research proposes the NetSc based strategy to attenuate interference in a given 5G heterogeneous network. The effect of this mitigation will improve the overall efficiency of the system. In this scheme, the cells are organized to obtain centre and terminal clusters. Each cell is assigned auxiliary band based on the NetSc algorithm. This design model is concerned with the reduction of interference around the small cells, thus, for each idle cluster; an active cell can use the sub-band around the terminals of the idle neighbouring cluster while reserving the remaining sub-band for the centre cluster. On the other hand, suppose the sub-band capacity is saturated by the terminal clusters, then each cluster of any small cell falls back to its own sub-band. Every small cell and corresponding macro cells can establish a network to share user equipment information and other measurements. The user equipment data and transmission rate are also made available to the router which takes decision on the small cell switching. Small cell sub-band assignment can be performed using Algorithm 1.

### Algorithm 1: Small cell sub-band Assignment

1: Begin

2: Initialize a collection of all possible sub-bands as  $S_B \leftarrow 0$

3: Initialize a collection of all small cells as  $U_{SC} \leftarrow 0$

4: Initialize a sub-band assigned to small cell as  $B_{SC}$

5: **for**  $l = 0; i < U_{SC}.length; i++$

6:     locate a collection of used sub-band in the terminal cluster of the surrounding small cells and store in a variable  $E_c$

7:     Compute a collection of the remnant sub-band for the terminal cluster of the active small cell as  $R_c = S_B - E_c$

8:     **if**  $R_c.length > 1$  **then**

9:         **for each** sub-band  $r$  in  $R_c$

10:             Compute the nearest distance as  $d_{min}$  between the sub-band allocated to the target small cell and the closest small cell using the sub-band  $r$  within its terminal cluster.

11:             Compute the sub-band with the maximum distance as  $r_{max}$

12:              $B_{SC} \leftarrow r_{max}$

13:         **end for**

14:     **else if**  $R_c.length = 1$

15:          $S_B \leftarrow R_c$

16:     **else**

17:         **for each** sub-band  $e$  in  $E_c$

18:             Compute the distance as  $d_e$  between the sub-band allocated to the target small cell and the surrounding small cell using the sub-band  $e$  within its terminal cluster.

19:             Compute  $e_{max}$  such that  $e$  has the maximum distance  $d_e$

20:              $B_{SC} \leftarrow e_{max}$

21:         **end for**

22:     **end if**

23: **end for**

Algorithm 1 can be segmented into two main categories which are: the determination of used sub-band in the terminal cluster of the surrounding small cells (line 6 and line 7) and determination of sub-band assigned to small cell (line 8 to line 20).

When any small cell is powered up, it detects its immediate surrounding small cell signal to obtain their sub-bands. This action is necessary by the newly powered small cell to avoid coincidental use of already used sub-band. Algorithm 1 identifies all used sub-bands and store them in an array denoted as  $E_c$  while the free sub-bands are stored in  $R_c$ . The algorithm iterates through  $R_c$  to obtain the closest sub-band and the smallest cell using it. If all available sub-bands are assigned to the terminal cluster in the surrounding small cells, then the sub-band used by the farthest surrounding small cell is selected in order to reduce interference. The Middle cluster has the privilege to use the remaining sub-bands. This assignment procedure is further depicted in Figure 2.

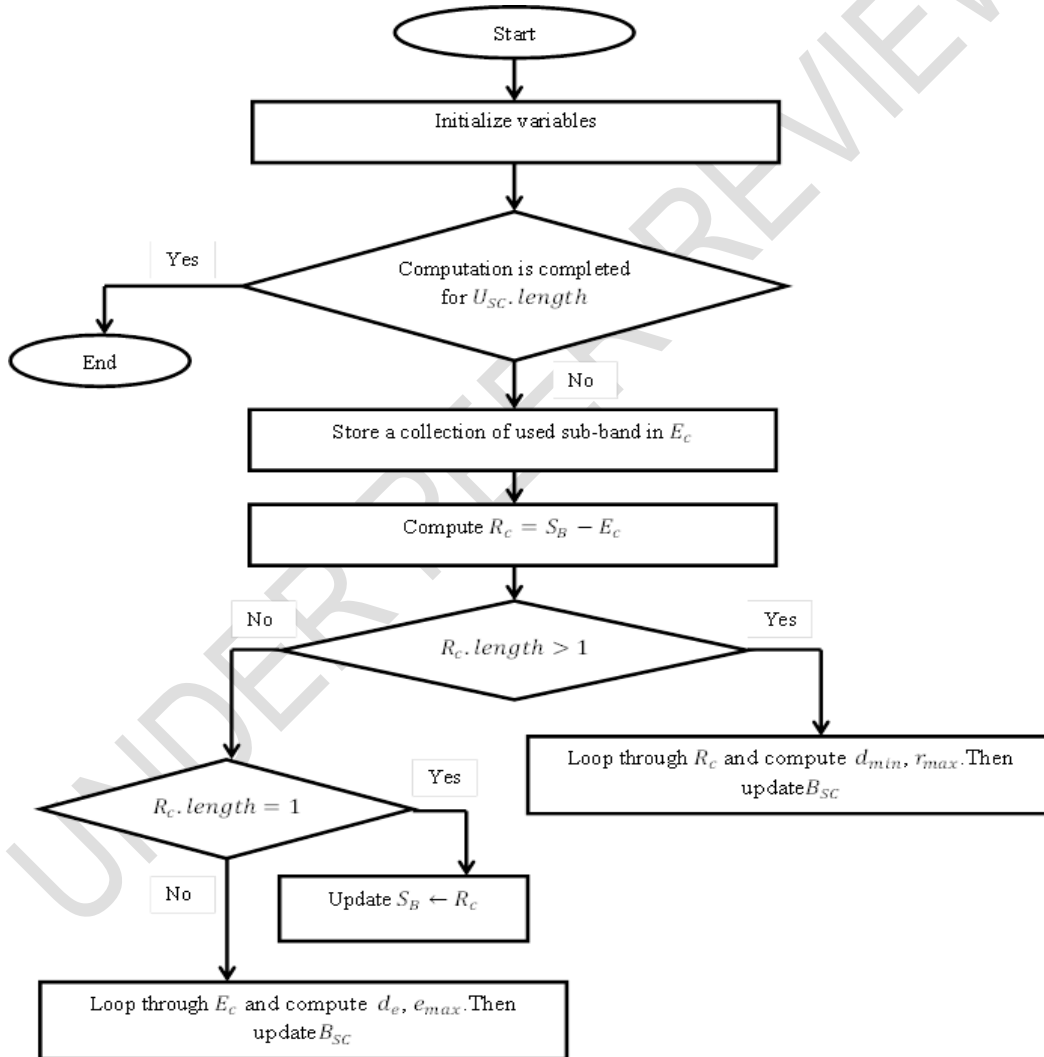


Figure2. Flowchart showing small cell sub-band assignment

### 2.3 Cluster Vertices Formation

The vertices of each cluster can be formulated to obtain either a circular-contoured cluster or an irregular-contoured cluster. The procedure for computation of middle cluster layout or contours and vertices is presented in Algorithm 2. The vertices of each cluster are constructed based on the cluster's radius. If the middle cluster has similar contour with the terminal cluster, then the radius of the middle cluster can be computed as a partial length between every vertex and the middle of the small cell. To formulate the layout of the middle cluster, one major criterion is to compute the contour parameters. This procedure of obtaining small cell vertex is performed for all the small cells whose vertices are to be determined. If the length between the vertex of the closest small cell and the middle is of another small cell is obtained, then the closest acceptable distance is obtained.

### Algorithm 2: Middle Cluster Determination Procedure

1: **Begin**

2: Define the collection of small cells as  $Z_{sc}$

3: Define the middle small cell coordinate as  $(x_{sc_{mid}}, y_{sc_{mid}})$

4: Define the coordinates of vertices as  $(x_{vert}, y_{vert})$

5: Define small cell radius as  $r_{sc}$

6: Define small cell vertex  $v_{sc}$

7: Initialize  $[\ ] \leftarrow Z_{sc}$

8: Initialize  $(0,0) \leftarrow (x_{sc_{mid}}, y_{sc_{mid}})$

9: Initialize  $(0,0) \leftarrow (x_{vert}, y_{vert})$

10: Initialize  $0 \leftarrow r_{sc}$

11: **For each**  $SC$  in  $Z_{sc}$

12:     **if** irregular-contoured cluster **then**

13:         **For each**  $v_{sc}$  in  $SC$

14:             Compute the length of each vertex  $l_v$  with respect to the middle of the small cell

15:             Compute the radius of the middle clustered small cell  $r_{mid} = r_{sc} \times l_v$

16:             Connect  $v_{sc}$  to middle  $SC$

17:             Compute  $(x_{sc_{mid}}, y_{sc_{mid}})$ : taken as the line intersection in Step 16

18:         **end for**

19:     **else if** circular-contoured cluster **then**

20:           **For each**  $v_{sc}$  in  $SC$

21:                     Compute the length of each vertex  $l_v$  with respect to the middle of  
                          the small cell

22:           **end for**

23:           compute the least  $l_v$

24:           compute  $r_{mid} = r_{sc} \times least l_v$

25:           Connect  $v_{sc}$  to middle  $SC$

26:           Compute  $(x_{sc_{mid}}, y_{sc_{mid}})$

27:       **end if**

28: **end for**

29: **end**

The middle cluster determination procedure presented in Algorithm 2 is further depicted in Figure 3.

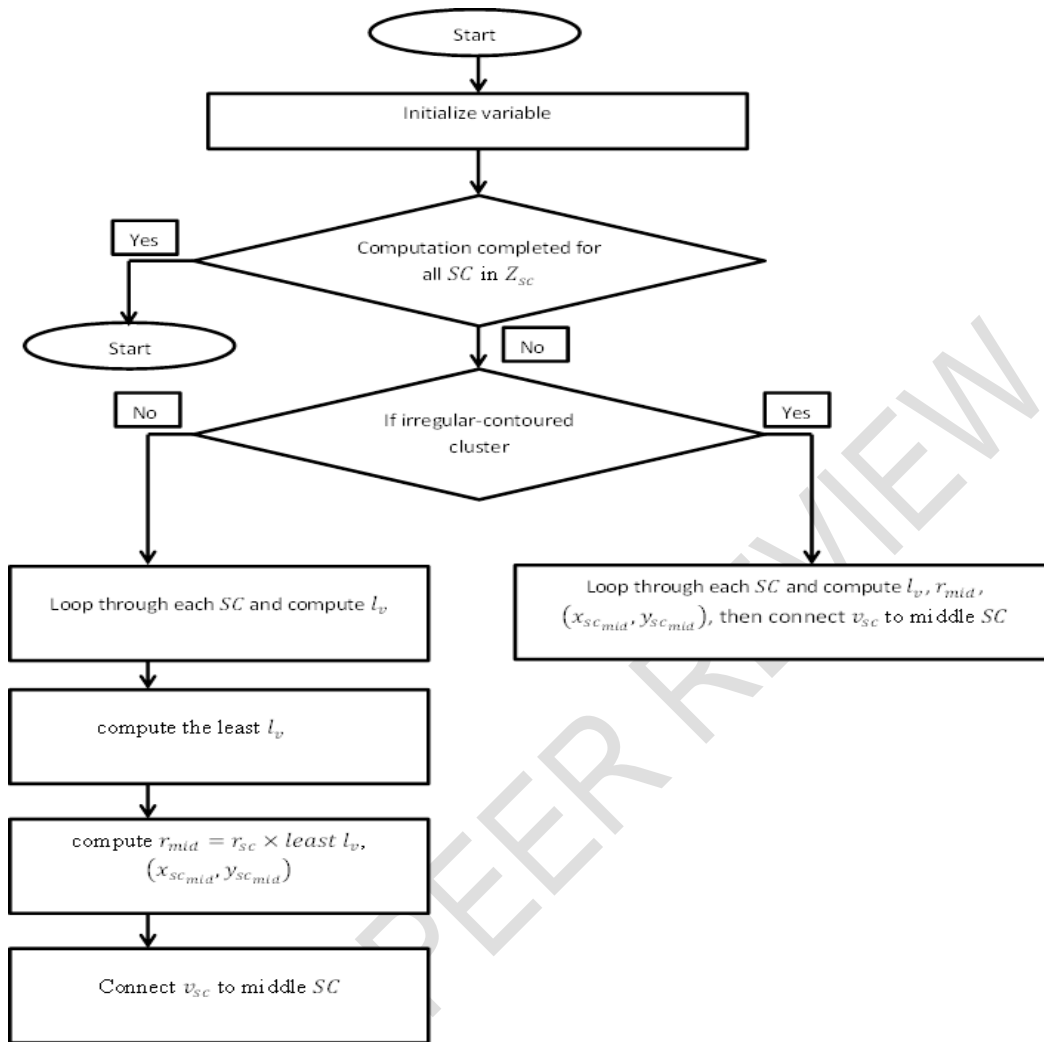


**Figure3. Flowchart for Middle Cluster Determination**

### 2.3 Power Consumption/Interference Management

In order to mitigate interference for cell edge users in 5G network using Network Cell Segmentation, power management is essential. In quest to keep power consumption of the system at barest minimum, this research adopts the small cell switching strategy. In this strategy, any small cell is switched on or off based on traffic and the rate of interference it produces. The small cell switching strategy is developed in Algorithm 3.

#### **Algorithm 3: Small Cell Switching Procedure**

- 1: Begin
- 2: Define the number of user equipment within small cell as  $N_{ue_{sc}}$
- 3: Define total load within small cell as  $L_{T_{sc}}$
- 4: Define load threshold within small cell as  $L_{THLD_{sc}}$

5: Defined maximum received signal strength in small cell as  $RSS_{max_{sc}}$

6: Define threshold received signal strength in small cell as  $RSS_{THLD_{sc}}$

7: Define the rate of interference produced by small cell as  $\psi_{sc}$

8: Define the average rate of interference produced by small cell as  $\bar{\psi}_{sc}$

9: Define a set of all small cells as  $Z_{sc}$

10: Define a set of all switched off cells as  $Z_{sc_{off}}$

11: Define a set of all switched on cells as  $Z_{sc_{on}}$

12: Define a set of all undefined state small cell as  $Z_{sc_u}$

13: Initialize  $0 \leftarrow N_{ue_{sc}}, L_{T_{sc}}, L_{THLD_{sc}}, RSS_{max_{sc}}, RSS_{THLD_{sc}}, \psi_{sc}, \bar{\psi}_{sc}$

14: Initialize  $[ ] \leftarrow Z_{sc}, Z_{sc_{off}}, Z_{sc_{on}}, Z_{sc_u}$

15: **For each**  $SC$  **in**  $Z_{sc}$

16: **if**  $N_{ue_{sc}} = 0$  **then**

17:      $Z_{sc_{off}} \leftarrow SC$

18: **else if**  $L_{T_{sc}} > L_{THLD_{sc}} \parallel RSS_{max_{sc}} > RSS_{THLD_{sc}}$  **then**

19:      $Z_{sc_{on}} \leftarrow SC$

20: **else**

21:      $Z_{sc_u} \leftarrow SC$

22: **end if**

23: **end for**

24: **For each**  $SC$  **in**  $Z_{sc_{on}}$

25:      $\psi_{total_{sc}} \leftarrow \psi_{sc}$

26: **end for**

27:  $\bar{\psi}_{sc} \leftarrow \psi_{total_{sc}} / Z_{sc_{on}}.Count$

28: **For each**  $SC$  **in**  $Z_{sc_u}$

29:     **if**  $\psi_{sc} > \bar{\psi}_{sc}$  **then**

```
30:         Execute line 17
31:     else
32:         Execute line 19
33:         Execute line 25
34:         Execute line 27
35:     end if
36: end for
37: end
```

In the small cell switching procedure presented in Algorithm 3, two major processes were highlighted. First, the state of all small cells was identified and each small cell was categorized based on state. There are three states in which small cell can be (one at a time). These states are “on”, “off”, and “undetermined”. The pictorial illustration of Algorithm 3 is presented in Figure 4.

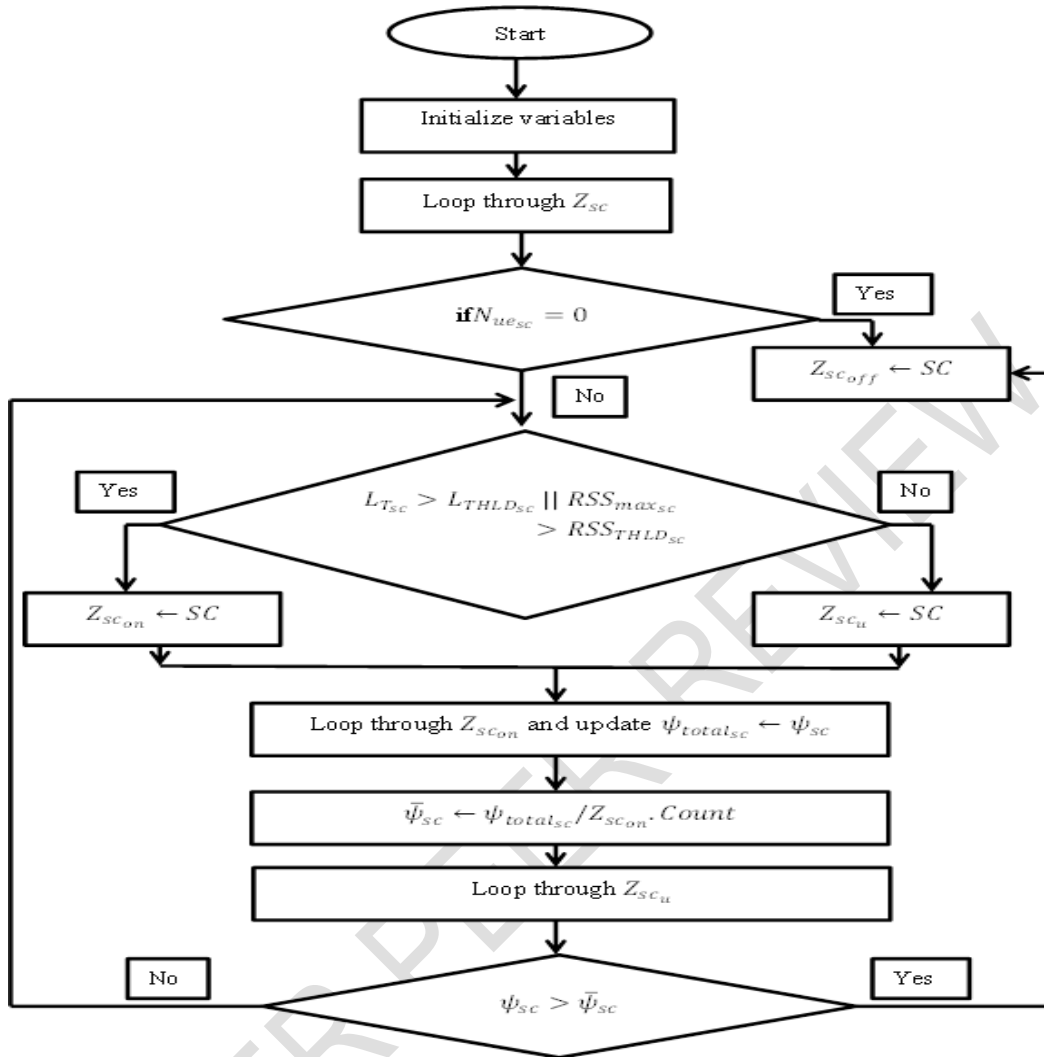


**Figure 4. Flowchart for Small Cell Switching Procedure**

The algorithm pushes any small cell into “off” state if the number of user equipment within it is zero, as shown from line 16 to line 17, otherwise the small cell is pushed into “on” state as shown from line 18 to line 19. If the state of the small cell cannot be determined at any given time, then the small cell is pushed to the collection of undetermined state small cells object seen from line 20 to line 21. Line 24 to line 26 computes the total interference level of all small cells in “on” state. Average interference level is computed in line 27.

Secondly, the algorithm further categorizes the small cells contained in the undetermined state object into “on” state and “off” state. The criteria the algorithm adopts for this categorization is based on the level of interference produced by the small cell. If the interference level in the small cell is greater than the average permissible interference level of all small cells in “on” state, then the cell is switched off, otherwise it is switched on. This cell state categorization is found from Line 28 to Line 33.

### 3. RESULTS AND DISCUSSION

#### 3.1 Performance Analysis of the Proposed Irregular-Contoured and the Proposed Circular-Contoured Middle Cluster

The overall data rate with respect to number of user equipment is presented in Table 2 and Figure 5.

**Table 2.** Data rate versus number of user equipment for circular-contoured cluster and irregular-contoured cluster

Number of user equipment	Data rate (kbps)	
	circular-contoured cluster	irregular-contoured cluster
100	1.32	1.02
200	2.36	2.15
300	3.40	3.18
400	4.42	4.22
500	5.48	5.27
600	6.51	6.32
700	7.55	7.36
800	8.59	8.41
900	9.63	9.46
1000	10.69	10.52

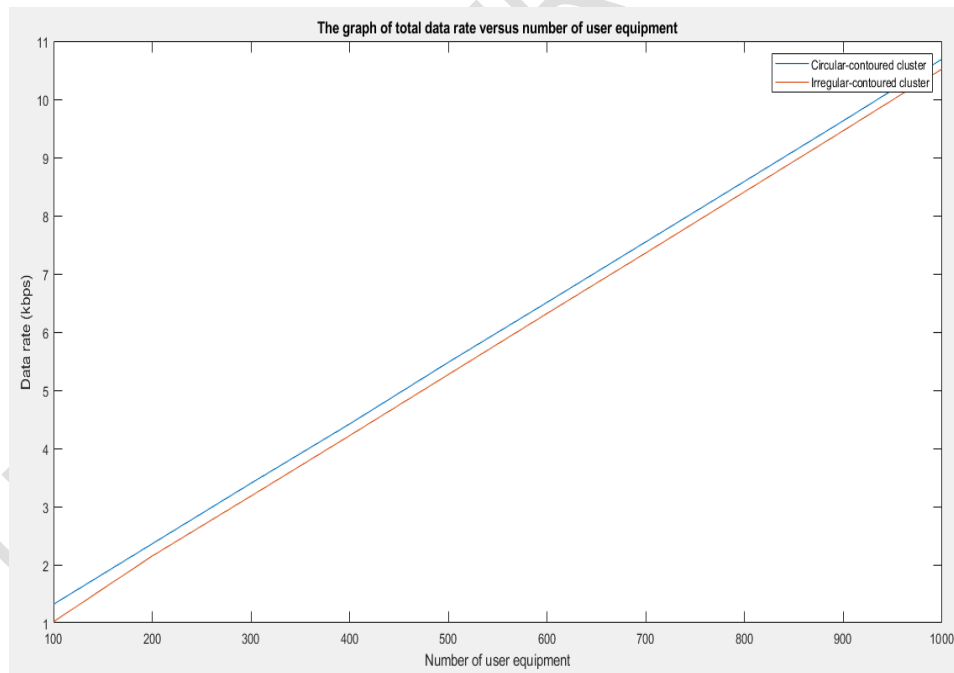


**Figure 5.** Data rate versus number of user equipment for circular-contoured cluster and irregular-contoured cluster

From the results obtained in table 2, an average data rate of 5.995 *kbps* was obtained for the circular-contoured cluster while 5.791 *kbps* was obtained for the irregular-contoured cluster. The circular cluster have actually improved the data rate batter than the irregular cluster.

Accordingly, the power consumption with respect to number of user equipment is computed and the results presented in Table 3 and Figure 6.

**Table 3. Power consumption versus number of user equipment for circular-contoured cluster and irregular-contoured cluster**

Number of user equipment	Power consumption (KW)	
	circular-contoured cluster	irregular-contoured cluster
100	1.30	1.28
200	1.35	1.32
300	2.00	1.97
400	2.50	2.48
500	3.00	2.87
600	3.52	3.48
700	4.10	4.07
800	4.51	4.49
900	5.20	4.98
1000	5.50	5.49

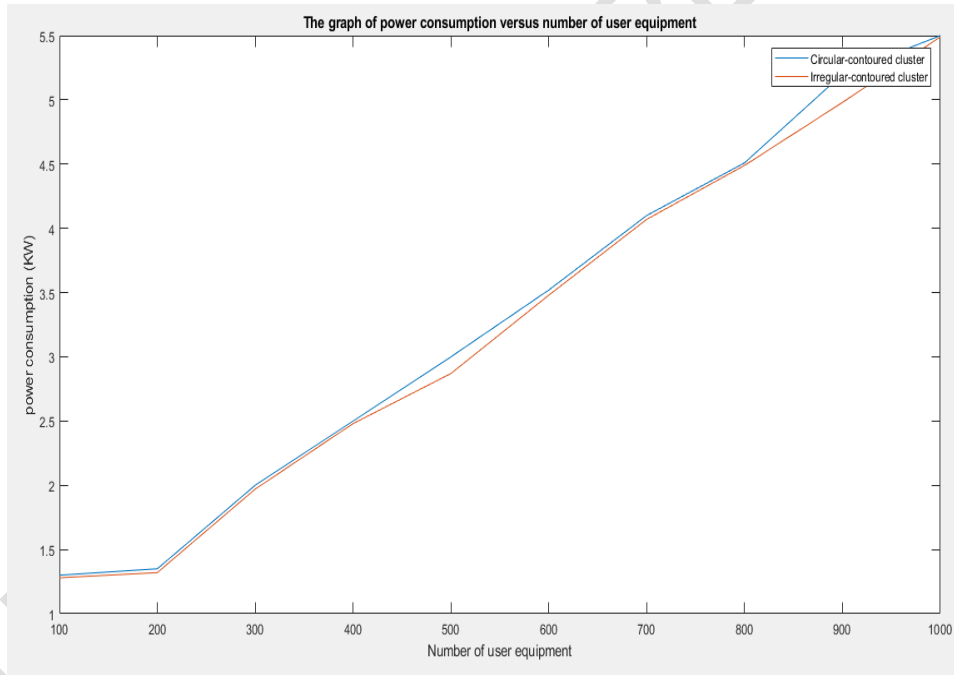


**Figure 6. Power consumption versus number of user equipment for circular-contoured cluster and irregular-contoured cluster**

The power consumption efficiency was estimated for various quantity of user equipment. Also, the failure probability for various signal-to-noise ratio which is computed as a portion of user equipment which cannot meet the threshold signal to noise ratio. The failure probability computation was done based on Equation 15.

$$\rho_{failure} = \frac{\sum_c \sum_j \lambda_{j,c} \cdot SNR_{j,c}}{\sum_c \sum_j \cdot SNR_{j,c}} \quad (15)$$

Subject to

$$\begin{cases} \lambda_{j,c} = 1; & \text{if } SNR_{j,c} < SNR_{threshold} \\ \lambda_{j,c} = 0; & \text{otherwise} \end{cases}$$

Table 4 and Figure 7 show that the circular-contoured cluster and the irregular-contoured cluster has close performance. This implies that the circular-contoured cluster model can be executed with confidence with Omni-directional antenna.

**Table 4. Power efficiency for circular-contoured cluster and irregular-contoured cluster**

Number of user equipment	Power efficiency (kbps/W)	
	circular-contoured cluster	irregular-contoured cluster
<b>100</b>	100	98
<b>200</b>	150	148
<b>300</b>	210	205
<b>400</b>	250	247
<b>500</b>	305	299
<b>600</b>	351	348
<b>700</b>	412	405
<b>800</b>	450	447
<b>900</b>	522	516
<b>1000</b>	551	549

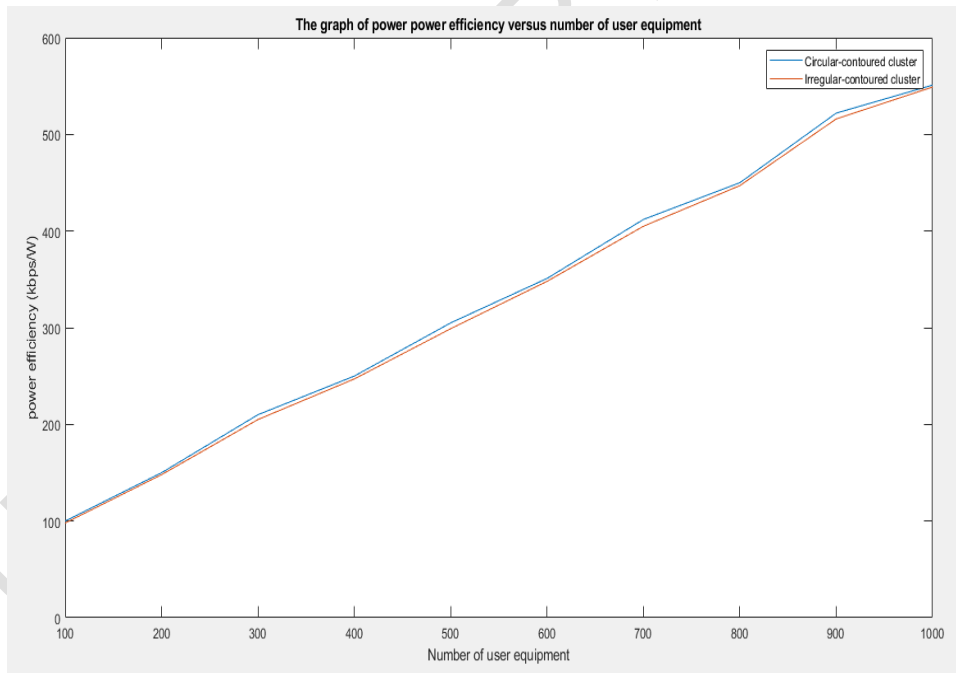


**Figure 7. Power efficiency for circular-contoured cluster and irregular-contoured cluster**

Also, the failure probability for circular-contoured and irregular-contoured cluster are presented in Table 5 and Figure 8.

**Table 5. Failure probability for circular-contoured cluster and irregular-contoured cluster**

Signal-to-noise ratio ( <i>dB</i> )	Failure probability	
	circular-contoured cluster	irregular-contoured cluster
<b>1</b>	0.10	0.12
<b>5</b>	0.15	0.17
<b>10</b>	0.30	0.32
<b>15</b>	0.51	0.52
<b>20</b>	0.72	0.73
<b>25</b>	0.84	0.84
<b>30</b>	0.91	0.93
<b>35</b>	0.96	0.95

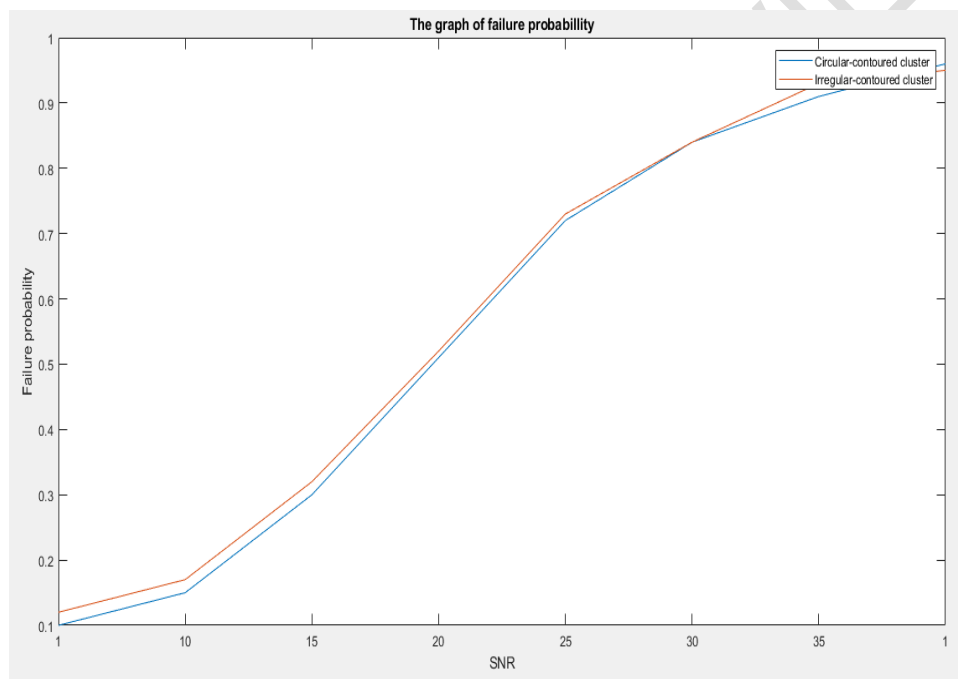


**Figure 8. Failure probability for circular-contoured cluster and irregular-contoured cluster**

An average power efficiency and average failure probability was computed, and 330.1 *kbps/W* and 0.5613 were obtained respectively, for circular-contoured cluster while 326.2 *kbps/W* and 0.5725 were obtained respectively for irregular-contoured cluster. The performance closeness of the two methods gives a high reliability on the circular-contoured cluster method.

### 3.2 Performance Analysis of Small Cell Switching Scheme

The power consumption of small cells was evaluated based on different user equipment and the results were compared with other schemes as shown in Table 6 and Figure 9. The results show that power consumption is a function of user equipment. This relationship exists

since transmission power becomes high if user equipment increases. The No SoftFrequencyReuse(NSFR) scheme developed by[1] consumes more power as shown in the results (Figure 9). This is because all the small cells simultaneously are active always. The soft frequency reuse (SFR) scheme developed by[4] consumes lower power compared to the NSFR scheme. This is because the SFR scheme is designed to allow low transmission power at the middle cluster. However, all small cells remain active always, thereby consuming more power. From Figure 9, the proposed scheme (Small Cell Switching Scheme) has the lowest power consumption. This is because small cells are turned off when they are idle or have a higher interference. Small cells are turned off due to high interference rate allocated to the user equipment within it to the nearest active small cell.

**Table 6. Power consumption versus number of user equipment**

Number of User Equipment	Power Consumption (KW)		
	NSFR scheme	SFR scheme	Proposed scheme
100	1.72	1.51	1.01
200	1.90	1.69	1.09
300	2.15	1.87	1.15
400	2.27	2.14	1.23
500	2.51	2.29	1.31
600	2.77	2.50	1.39
700	3.01	2.72	1.47
800	3.24	3.02	1.55
900	3.50	3.22	1.63
1000	3.73	3.51	1.72

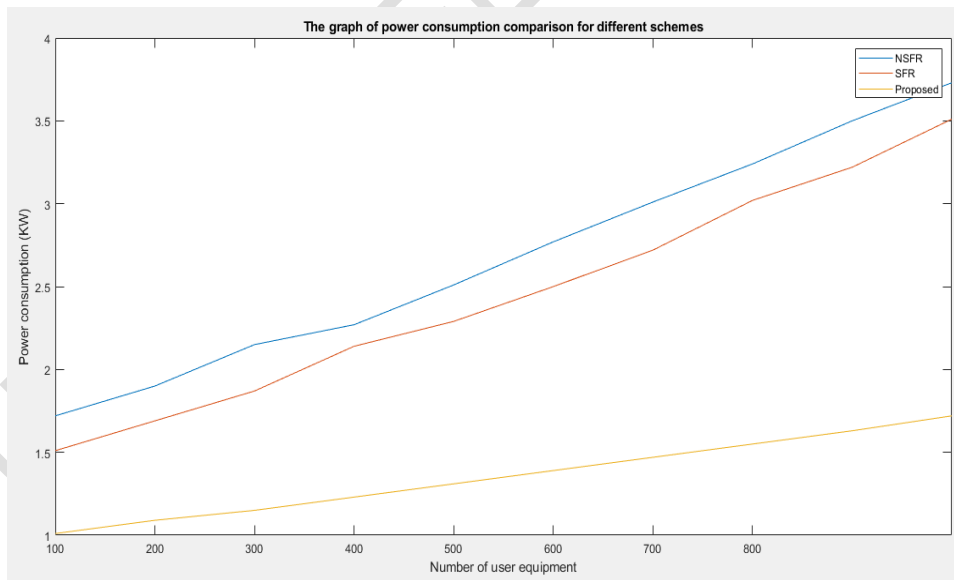


**Figure 9. Power consumption versus number of user equipment**

Table 7 and Figure 10 shows the system data rates with respect to user equipment. The results show that the proposed scheme has the highest data rate as the interference level is lowest here. On the other hand, the NSFR scheme has the least data rate and the highest interference level.

**Table 7. Data rate comparison for various schemes**

Number of User Equipment	Data Rate (kbps)		
	NSFR scheme	SFR scheme	Proposed scheme
100	1.72	1.92	2.82
200	2.76	3.05	3.95
300	3.80	4.08	4.88
400	4.82	5.12	6.02
500	5.88	6.17	7.08
600	6.91	7.22	8.13
700	7.95	8.26	9.17
800	8.99	9.31	10.22
900	10.03	10.36	11.28
1000	11.09	11.42	12.19

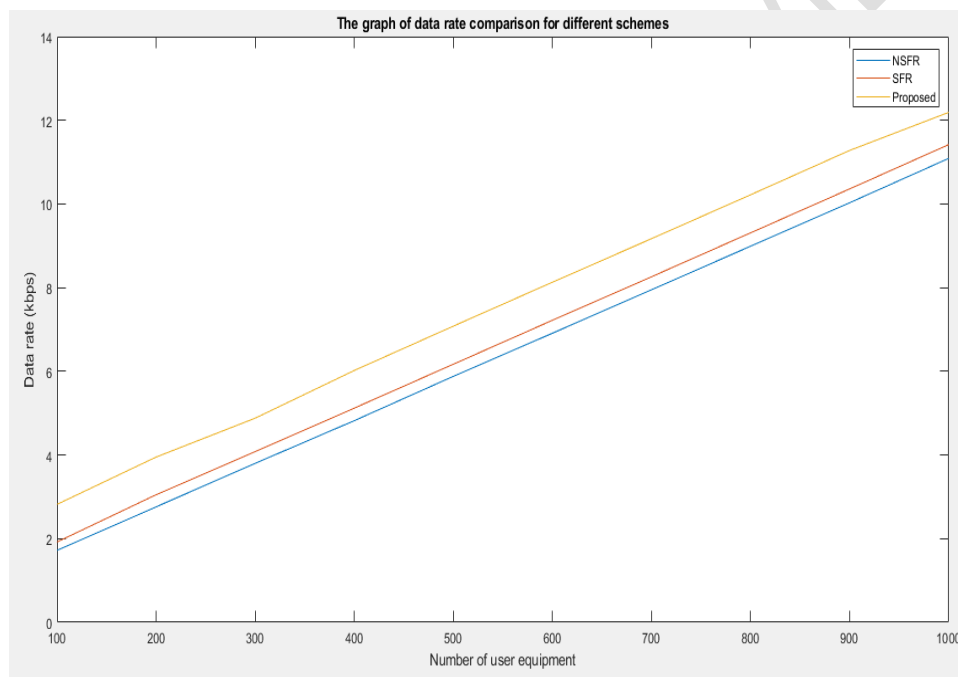


**Figure 10. Data rate comparison for various schemes**

The results in Figure 8 show the power consumption of various schemes. It is necessary to evaluate the power efficiency of these schemes. Hence, the result showing the power efficiency of each of the considered scheme is presented in Table 8 and Figure 11.

**Table 8. Power efficiency comparison of various schemes**

Number of User Equipment	Power Efficiency (kbps/W)		
	NSFR scheme	SFR scheme	Proposed scheme
100	108	112	152
200	158	160	202
300	215	227	264
400	257	270	302

<b>500</b>	310	322	363
<b>600</b>	359	370	405
<b>700</b>	418	429	472
<b>800</b>	459	470	505
<b>900</b>	527	538	580
<b>1000</b>	560	572	610

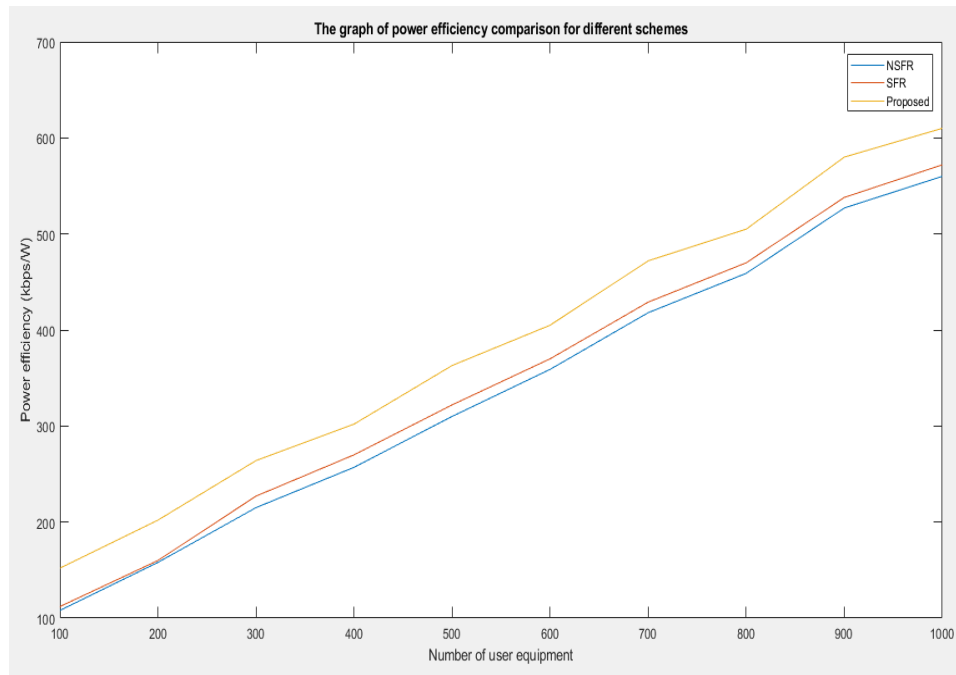


**Figure 11. Power efficiency comparison of various schemes**

A comparative analysis of power consumption, data rate and power efficiency were performed between NSFR model, SFR model and the proposed model. The results show that the proposed model has low power consumption compared to other two methods, and consequently, high data rate which implies that the interference level is low, and with a high-power efficiency. The results presented in Figure 10 show that the interference mitigation handled by the proposed scheme improves by about 22%.

#### 4. CONCLUSION

The implications of cluster formation have been extensively analyzed in this research. Specifically, two categories of these formations were considered namely: circular-contoured cluster and irregular-contoured cluster. Although the irregular-contoured cluster does not have realistic implementation, its application to this research is based on theoretical perspective and to be used as a benchmark tool for a more realistic solution. On the other hand, circular-contoured clustering technique – a more realistic approach in terms of implementation is presented in this research. Various metrics were used to measure the comparative performances of these two methods.

From the results, an average data rate of 5.995 *kbps* was obtained for the circular-contoured cluster while 5.791 *kbps* was obtained for the irregular-contoured cluster. An average power

consumption of 3.298 *KW* was obtained for the circular-contoured cluster and 3.243 *KW* was obtained for the irregular-contoured cluster model. Similarly, average power efficiency and average failure probability was computed, and 330.1 *kbps/W* and 0.5613 were obtained respectively, for circular-contoured cluster while 326.2 *kbps/W* and 0.5725 were obtained respectively for irregular-contoured cluster. The performance closeness of the two methods gives a high reliability on the circular-contoured cluster method.

The NSFR model, SFR model, and the suggested model were compared in terms of power efficiency, data rate, and consumption. The findings demonstrate that, in comparison to the other two ways, the suggested model consumes less power and, as a result, has a high data rate, indicating a low degree of interference, and a high-power efficiency. The data displayed in Figure 10 demonstrate a 22% improvement in the interference mitigation managed by the suggested system.

## REFERENCES

- [1] H. Fourati, R. Maaloul and L. Chaari, "A survey of 5G network systems, challenges and machine learning approaches," *International Journal of Machine Learning and Cybernetics*, pp. 385-431, 2021.
- [2] A. Oloyede, S. Ozuomba and C. Kalu, "Shibuya Method for Computing Ten Knife Edge Diffraction Loss," *Software Engineering*, vol. 5, no. 2, pp. 38-43, 2017.
- [3] O. Simeon, "Analysis Of Effective Transmission Range Based On Hata Model For Wireless Sensor Networks In The C-Band And Ku-Band," *Journal of Multidisciplinary Engineering Science and Technology*, vol. 7, no. 12, pp. 13673-13679, 2020.
- [4] M. Dee Ree, G. Mantas, A. Radwan, S. Mumtaz, J. Rodriguez and I. Otung, "Key Management for Beyond 5G Mobile Small Cells: A Survey," *IEEE Access*, vol. 7, pp. 59200-59236, 2019.
- [5] A. Andrae and T. Edler, "On Global Electricity Usage of Communication Technology: Trends to 2030," *Challenges*, vol. 6, no. 1, pp. 117-157, 2015.
- [6] S. Sheikhzadeh and M. Javan, "Key Technologies in 5G: Air Interface," *MODARES JOURNAL OF ELECTRICAL ENGINEERING*, vol. 16, no. 2, pp. 50-61, 2016.
- [7] V. Wong, R. Schober, W. Ng and L. Wang, *Key technologies for 5G wireless systems*, Cambridge, U.K.: Cambridge University Press, 2017.
- [8] N. Al-Falahy and O. Alani, "Technologies for 5G Networks: Challenges and Opportunities," *IT Professional*, vol. 19, no. 1, pp. 12-20, 2017.
- [9] V. Stoyanov, V. Poulkov, G. Iliev and P. Koleva, "Ultra-Dense Networks: Taxonomy and Key Performance Indicators," *Symmetry*, vol. 15, no. 1, 2022.
- [10] W. Yu, H. Xu, H. Zhang, D. Griffith and N. Golmie, "Ultra-Dense Networks: Survey of State of the Art and Future Directions," in *25th International Conference on Computer Communication and Networks (ICCCN)*, California, 2016.
- [11] M. Usama, "A Survey on Recent Trends and Open Issues in Energy Efficiency of 5G," *Sensors*, vol. 19, no. 14, p. 3126, 2018.
- [12] C. Liu, B. Natarajan and H. Xia, "Small Cell Base Station Sleep Strategies for Energy Efficiency," *IEEE Transactions on Vehicular Technology*, vol. 65, no. 3, pp. 1652-1661, 2016.
- [13] B. Shen, Z. Lei, X. Huang and Q. Chen, "An Interference Contribution Rate Based Small Cells On/Off Switching Algorithm for 5G Dense Heterogeneous Networks," *IEEE Access*, vol. 6, no. 1, pp. 29757-29769, 2018.

- [14] L. Huo, D. Jiang and Z. Lv, "Soft frequency reuse-based optimization algorithm for energy efficiency of multi-cell networks," *Computers & Electrical Engineering*, vol. 66, pp. 316-331, 2018.

UNDER PEER REVIEW